ACS APPLIED MATERIALS & INTERFACES

RESEARCH ARTICLE

www.acsami.org

Cellulose Nanocomposite Biopolymer Foam—Hierarchical Structure Effects on Energy Absorption

Anna. J. Svagan,*,† Lars A. Berglund,*,† and Poul Jensen‡

†Wallenberg Wood Science Center and Department of Fibre and Polymer Technology, Royal Institute of Technology, SE-100 44 Stockholm, Sweden, and

‡National Museum Denmark, DK-2800 Lyngby, Denmark

ABSTRACT: Starch is an attractive biofoam candidate as replacement of expanded polystyrene (EPS) in packaging materials. The main technical problems with starch foam include its hygroscopic nature, sensitivity of its mechanical properties to moisture content, and much lower energy absorption than EPS. In the present study, a starch-based biofoam is for the first time able to reach comparable mechanical properties (E = 32 MPa, compressive yield strength, 630 kPa) to EPS at 50% relative humidity and similar relative density. The reason is the nanocomposite concept in the form of a cellulose nanofiber network reinforcing the hygroscopic amylopectin starch matrix in the cell wall. The biofoams are prepared by the freezing/freeze-drying technique and subjected to compressive loading. Cell structure is characterized by FE-SEM of cross sections. Mechanical properties are related to cell structure and cell wall nanocomposite composition. Hierarchically structured biofoams are demonstrated to be interesting materials with potential for strongly improved mechanical properties.

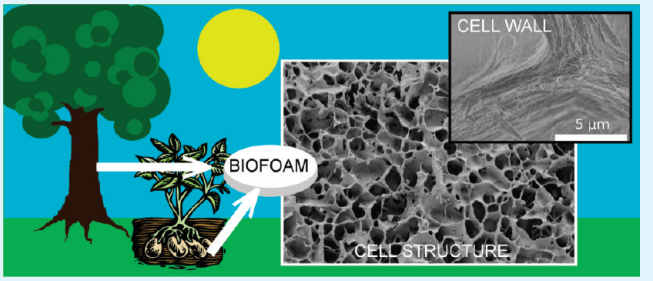

KEYWORDS: starch, cellulose nanofibers, biofoam, mechanical properties, packaging applications

INTRODUCTION

Biopolymer foams from renewable resources are of interest as replacement of petroleum-based polymer foams. The potential functions of biofoams include thermal insulation, impact energy absorption in packaging materials or in crash protection, mechanically robust core materials in sandwich structures, or as soft foams with cushioning function in car seats. In addition, the area of use spans to biomedical applications such as scaffolds for tissue engineering or implants for bone substitution where mechanical function and cell size control of the foam are critical. In food science, bread and related products can be viewed as structural biofoam materials. Here the mechanical properties are relevant for our perception of the food, for instance, its "crispness".[1]

Expanded polystyrene (EPS) foam is a well-known large-scale application of petroleum-based polymers. This foam is often of white color and is used as impact-absorbing packaging material for microelectronics consumer products such as computers and DVD players. According to statistics for the year 2007, the global market for EPS was over 4×10^9 kg.[2] Because EPS foams may have a density as low as 15 kg m^{-3}, the volume of the annual consumption is difficult to even envision. The EPS waste problem is significant.

Starch biofoam is a promising alternative for EPS, because starch is biodegradable and originates from renewable resources. The main technical challenges with starch biofoam comprise its hygroscopic nature and a much lower energy absorption and strength in compression compared with EPS at similar relative density. The reason for lower mechanical performance is the reduction of cell wall properties even at ambient conditions, due to moisture sorption. Moisture plasticizes the starch cell wall so that the glass-transition temperature, Young's modulus, and strength are significantly reduced.[3,4] Additionally, the cell structure of starch foams is not always ideally suited for maximum mechanical performance.

Building on earlier work by Dufresne et al.,[4−6] we recently managed to prepare high mechanical performance cellulose nanocomposite films based on amylopectin starch (PAP).[7] The starch matrix was plasticized by glycerol in order to mimic the anticipated effect of water in service. Despite the soft matrix with a Young's modulus typical of a rubber, $E_s \approx 1.6$ MPa, the material with 70 wt % cellulose nanofiber content showed a Young's modulus of 6.2 GPa and a tensile strength of 160 MPa. This is due to the nanofiber reinforcement in the shape of microfibrillated cellulose (MFC) from wood pulp fibers.[8] MFC obtained through disintegration of wood pulp fibers, usually has a lateral dimension in the range 15−30 nm and a length of several micrometers. The cellulose nanofibers are typically in aqueous suspension prior to preparation of nanocomposites. Because the cellulose crystal has a longitudinal Young's modulus of 134 GPa, the modulus and strength of the nanofibers are expected to be high. A key factor is that the cellulose nanofibers can form a strong network structure in the matrix material.[4−7,9] As a consequence, softening of a starch matrix surrounding a cellulose nanofiber network is not catastrophic to the mechanical performance of the nanocomposite.

Received: April 21, 2010
Accepted: March 31, 2011
Published: April 26, 2011

Instead, an attractive combination of modulus, tensile strength, ductility, and work to fracture is obtained.[7] The molecular interaction between cellulose and amylopectin starch is favorable because the chemical structure characteristics show similarities. This facilitates MFC dispersion in the PAP-water solution, and also promotes positive nanofiber−matrix interaction.[7]

The experience from MFC-starch films inspired a short communication, where nanocomposite biofoams were successfully prepared based on amylopectin starch and cellulose nanofibers.[10] Although mechanical performance was improved, the potential in terms of crushing strength (scales with energy absorption) was far from realized. To improve mechanical performance, we need to combine the nanocomposite structure of the cell wall with controlled cellular structure. For instance, a foam with much enhanced mechanical properties was expected at 70 wt % MFC content in the PAP cell wall. However, the cell structure was highly unfavorable and thus the energy absorption characteristics were very low.

For cellulose nanocomposite biofoams to compete with EPS, it is necessary to develop preparation methods that provide better control of the cell structure. The freezing/freeze-drying technique is of interest for biomedical applications,[11−13] but can also be justified for other high-technology applications[14] and as a method for manufacturing model materials. For instance, because it is possible to independently control cell wall composition and cellular structure, these model materials can be used to study hierarchical structure effects in biofoams. The preparation starts with a water suspension containing (here) cellulose nanofibers and "dissolved" amylopectin starch. This suspension is frozen. As the ice crystals are nucleated and growing, PAP and MFC is pushed to the interstitial regions between the numerous ice crystals.[15] The ice crystal size is controlled by, among other parameters, the freezing temperature. The cell shape is influenced by the predominant direction of heat flow and the kinetics of ice crystal growth.[16,17] Next, in the freeze-drying step, the ice is sublimated at a subzero temperature and voids appear where the ice crystals were located. In a previous study, we found that cell structure alteration during sublimation is a problem, but can be avoided by selection and control of the freeze-drying temperature.[18] This study allowed strongly improved cell structure control for tailoring of a hierarchical biofoam structure. The present work reports on cellular and cell wall structure and mechanical energy absorption of cellulose nanocomposite biofoams subjected to uniaxial compression. An important objective is to assess whether cell wall reinforcement of starch by MFC combined with cellular structure control can demonstrate the potential of MFC-starch biofoams as replacement of EPS.

EXPERIMENTAL SECTION

Microfibrillated Cellulose (MFC) Preparation. The 2 wt % MFC suspension in deionized water was prepared as described previously.[18] In short, it was obtained by treating never-dried bleached sulphite pulp from spruce (Nordic Paper Seffle AB, Säffle, Sweden) in four steps: mechanical beating, enzymatic treatment (enzyme Novozym 476, Novozymes A/S, Denmark), mechanical beating, and finally high-pressure homogenization. The dry pulp had a hemicellulose content of 13.8 wt % and a lignin content of 0.7 wt %. The average degree of polymerization (DP) of the cellulose in the MFC was estimated to 1700 ± 100 from four average intrinsic viscosity measurement values.[18]

Foam Preparation. Foams were obtained as follows. Suspensions containing amylopectin starch from potato (PAP, amylose content less than 1%, Lyckeby Stärkelsen, Kristianstad, Sweden), MFC and deionized water were mixed and simultaneously heated (water bath at 95 °C), see ref 18 for details. Cylindrical polystyrene Petri dishes (4.8 cm in diameter and 1.3 cm in height) were filled with suspension, degassed, refrigerated (8 °C) overnight, and finally frozen in one of three different ways: on the shelf in a freezer operating at −27 °C, on dry ice plates (CO_2(s), − 78 °C) placed in a freezer at −80 °C, or by keeping the bottom of the Petri dish in contact with liquid nitrogen (− 196 °C). Frozen samples were freeze-dried (5 weeks) in a Heto Powerdry freeze-dryer (PL9000) operating at a chamber pressure of 0.005 mbar. The sample temperature during freeze-drying was maintained slightly below or at −29 °C for 27 days and then gradually raised, over a period of eight days, to a value slightly above 0 °C.

Mechanical Testing. The compression testing was performed with an Instron 5566, using a load cell of 500 N or 5 kN. The cylindrically shaped foam was cut into cube specimens with a side of ca. 12 mm. The compression rate of the cross-head was set to 10% of the initial specimen height per min. Prior to testing, the specimens were stored for 8 days in a desiccator containing drying agent (silica gel, SiO_2, Sigma-Aldrich) and afterward conditioned at 51%RH and 23 °C for 3 days. The cubes were compressed in the direction parallel to the cylinder axis of the original foam. The compression test was performed at 51%RH and 23 °C. The displacement was measured using an Instron noncontacting video extensometer. Compressive stress−strain curves were plotted and the Young's modulus was determined from the slope of the low strain region. The yield strength of the test specimens was obtained by fitting one line each to the linear−elastic region and the cell collapse plateau of the compressive stress−strain curves. The intercept of the two fitted lines was taken as the yield point. The energy absorbed per unit volume at a certain peak stress, was obtained by calculating the area under the stress−strain curve up the peak stress. Mechanical compression data were averaged over five specimens.

Density Measurements. The foam density was calculated from the sample weight divided by the sample volume. The dimensions of the samples were measured using a digital caliper. Three measurements were made of each dimension. The porosity was obtained from $1 - [\rho^*/\rho_s]$, where ρ^* is the foam density and ρ_s is the cell wall density. The cell wall density was approximated as the theoretical density of the cell-wall, ρ_t, which was calculated from the densities, ρ_i, of the cell-wall constituents, i, and their weight fractions, W_i:

$$\rho_s \approx \rho_t = \frac{1}{\sum_{i=1}^{n} (W_i/\rho_i)} \quad (1)$$

The densities used in the calculation of ρ_t were 1260, 1500, and 1000 kg/m^3 for amylopectin,[7] MFC,[19] and water, respectively.

Foam Structure Analysis. Two Hitachi field-emission scanning electron microscopes (s-4300 and s-4800) were used to acquire secondary electron images of the foam morphology. Samples were sputter-coated with either gold, carbon, gold/palladium or a combination of gold/palladium and carbon. In cell wall observations, dry foam pieces were frozen in liquid nitrogen and bent to fracture using forceps. Samples for cell structure analysis were prepared by cutting foams with an UV excimer laser (wavelength 248 nm, irradiation energy 300 mJ/cm^2, 2 or 4 Hz, gas mixture of krypton and fluorine). Two adjacent samples was used to measure cell dimensions; one sample was used to study the plane normal to the cylinder axis and the other sample revealed the plane in the direction of the cylinder axis. In all foams, the two samples were removed from the area located at approximately the same (relative) radial distance to the cylinder axis. The image analysis software ImageJ (Research Services Branch, NIH, Bethesda, Maryland, USA) was used to measure the cell wall thickness and the three principal cell diameters. The cells were approximated as triaxial ellipsoids of constant shape. To account for the effect that the cells were not sectioned through

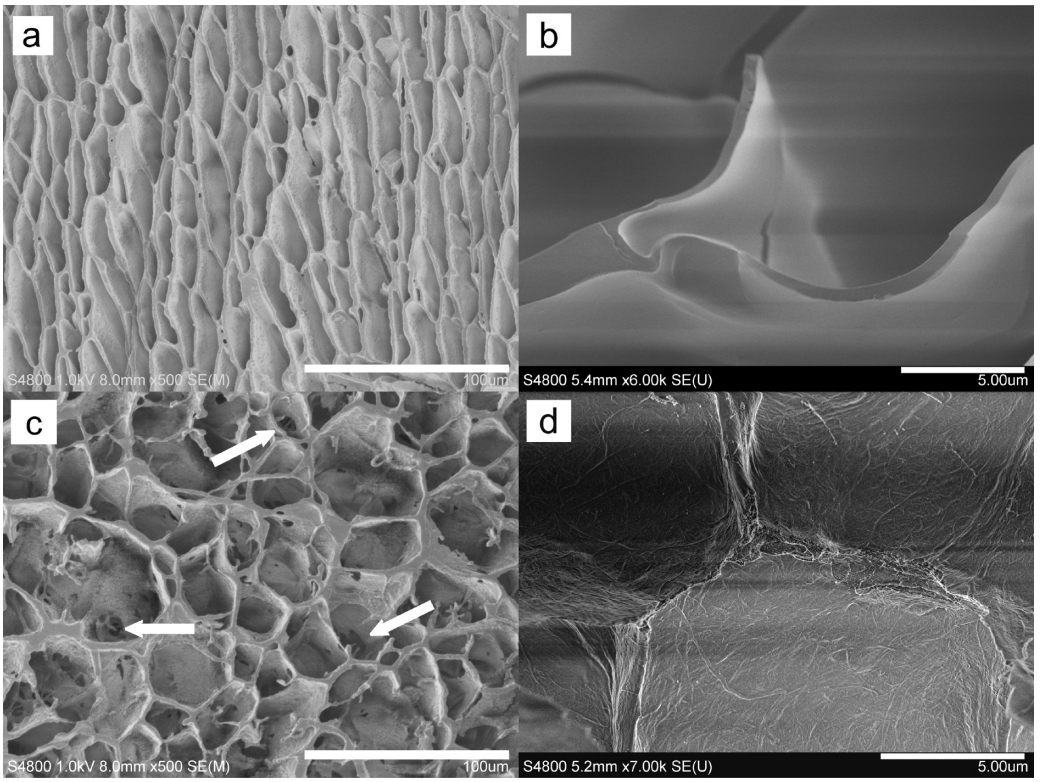

Figure 1. FE-SEM microscopy images of (a, b) neat amylopectin starch foam and (c, d) a composite foam with 40 wt % MFC in the cell wall. Images show (a, c) the cell structure and (b, d) the structure of the cell wall. Holes present in the cell walls of the composite foam are indicated by white arrows. Note the hierarchical structure of the composite foam. The scale bars are (a, c) 100 and (b, d) 5 μm.

their maximal cross-section, we obtained the mean cell diameters from[20]

$$\overline{L_1} = \frac{\pi}{2\overline{Z_1}} \text{ and } \overline{L_i} \approx \frac{\pi}{2\overline{Z_i}}, i = 2, 3. \quad (2)$$

where i stands for one of the three orthogonal axes in the triaxial ellipsoid and $\overline{Z_i}$ is the average value of Z_i, which is the reciprocal of the diameter in direction i on an elliptical section normal to one of the other two axes. The sample-sizes used in the calculations of $\overline{Z_i}$ and the estimated mean cell wall thickness ($\overline{T}$) were ca. 350 and 70, respectively. For all estimates, $\overline{X}$, the probability is equal or greater than 99%, that the error made in estimating the population mean, $\bar{x}$, by $\overline{X}$ is less than or equal to $0.1\,\overline{X}$, i.e., $P(|\overline{X}-\bar{x}| \leq 0.1\overline{X}) \geq 99\%$.

Water Content. The water content was calculated by dividing the weight loss of the conditioned sample by the sample weight prior to drying. The samples were dried overnight at 60 °C, followed by 3 h at 105 °C.

RESULTS AND DISCUSSION

Foam Morphology. In Figure 1a and 1b, FE-SEM images of the cell structure and cell wall are given for a pristine starch foam. In images c and d in Figure 1, the structure found in a 40 wt% MFC composite biofoam is presented. Clearly, these foams show a hierarchical structure with nanocomposite structure at the cell wall scale in addition to the cell structure at the micrometer scale. The cell structure given in Figure 1c and the cell wall depicted in Figure 1d represent characteristic images of the cell morphology found in cellulose nanofiber reinforced starch based biofoams. In composite foams, a fraction of the cells are open. In Figure 1c, the holes in the cell wall of the 40 wt % MFC biofoam are indicated by white arrows. By careful investigation, the cellulose nanofibers can be seen, see Figure 1d.

The fine scale of the cellulose nanofiber is an important factor in the reinforcement of cell walls of thicknesses in the micrometer range. Cellulose nanofibers of 15−40 nm diameters may be compared to wood pulp fibers with diameters typically of 20−30 μm. Pulp fiber reinforcement will strongly distort the cell structure of polymer foams and are unlikely to reinforce the cell wall polymer by efficient mechanisms. The width of the cellulose nanofibers was usually about 30 nm, although larger entities could also be observed. This is consistent with cellulose microfibril aggregates present in wood pulp fibers, as discussed by Iversen et al.[21] Typical lengths are in the micrometer scale. A homogeneous dispersion of nanofibers in the cell wall was observed in all foam types. In Figure 1, the cell wall found in the neat starch foam can be compared with that in the 40 wt % MFC biofoam. The importance of homogeneous dispersion cannot be exaggerated, and it is critical to the mechanical performance of the cell wall during the mechanical deformation of the biofoams.[22]

In Table 1, the anisotropy ratios, the type of cell structure (open or closed) and estimates of the mean cell diameters and mean cell wall thicknesses are summarized for foams of varying MFC content, 0−70 wt %, preparation temperatures (−27, −78, −196 °C) and porosity. In general, cell size is quite small and this is favorable from the point of view of failure properties. The data were collected from planes normal to and in the direction of the cylinder axis, at approximately half the height of the original foams. In the evaluation of the mechanical properties of the different foam types, we utilize the estimated mean cell diameter data in Table 1 as

Table 1. Estimates of the Mean Cell Diameters ($\overline{L_1}$, $\overline{L_2}$, $\overline{L_3}$) and Mean Cell Wall Thickness ($\overline{T}$) for Dry Composite Foams with Varying Cell Wall Composition, Preparation Temperatures, and Porosity[a]

preparation T (°C)	MFC content (wt %)	porosity (%)	$\overline{L_1}$ (μm)	$\overline{L_2}$ (μm)	$\overline{L_3}$ (μm)	$\overline{T}$ (μm)	$R_{12} = \overline{L_1}/\overline{L_2}$	$R_{13} = \overline{L_1}/\overline{L_3}$	open/closed cells
			Varying Cell Wall Composition (MFC/PAP)						
−78	0	91.8	44[b]	37[c]	18[c]	1.7[c]	1.2	2.4	closed
	10	92.1	42[c]	32[b]	15[b]	1.5[b]	1.3	2.8	both types
	30	92.0	54[c]	43[b]	23[b]	1.7[b]	1.2	2.3	both
	40	92.9	63[c]	59[b]	40[b]	2.5[b]	1.1	1.6	both
	60	93.2	99[c]	92[b]	57[b]	3.4[b]	1.1	1.7	both
	70	93.9							
			Varying Preparation Temperatures						
−27	30	91.9	99[b]	95[c]	56[b]	4.2[b]	1.0	1.8	both
−78	30	92.0	54[c]	43[b]	23[b]	1.7[b]	1.2	2.3	both
−196	30	91.9	30[c]	20[b]	14[b]	1.5[b]	1.5	2.1	both
			Varying Foam Porosity						
−78	30	96.3							
	30	92.0	54[c]	43[b]	23[b]	1.7[b]	1.2	2.3	both
	30	88.9	40[c]	37[b]	24[b]	2.5[b]	1.1	1.7	both

[a] R_{12} and R_{13} are the anisotropy ratios and the type of cells present in the foam is reported (closed and/or open). [b] Values obtained from sections normal to the cylinder axis. [c] Values obtained from sections in the direction of the cylinder axis. All studied areas were located at approximately half the height of the original foams. Data after Svagan et al.[18]

approximate values for the mean cell diameters of the entire foam cell population.

The largest estimate of the mean cell diameter, $\overline{L_1}$, in Table 1 was obtained in the direction of the predominant direction of the heat flow during freezing, which was primarily in the direction of the cylinder axis of the original foams. However, for the neat amylopectin starch foam, the largest diameter was obtained in the plane normal to the cylinder axis. This was probably because the sample was positioned close to the Petri-dish wall, where the wall influenced the heat flow direction.

By raising the MFC content in the cell wall, the estimates of the mean cell sizes and anisotropy ratios generally increased and decreased, respectively, see experimental data in Table 1. Additionally, a greater mean cell wall thickness was observed at higher MFC contents. Only the 10 wt % MFC foam did not follow the trend perfectly. The larger mean cell sizes, obtained by reducing the starch fraction in the cell wall, are considered to be a consequence of the inherent properties of starch. From previous investigations, it is known that highly water plasticized starch is transformed into a glassy state at subzero temperatures.[18,23] When the suspensions are frozen, this transition is considered to offer significant resistance to ice crystal growth. It is hypothesized that the size of the ice crystals when growth ceases, depends on the initial starch/water ratio in the suspension.[18] This could explain why larger cells appear in foams with lower starch content in the cell wall. It could also explain the smaller cell size with reduced porosity; compare mean cell sizes of 30 wt % MFC foams with porosities 88.9 and 92.0% in Table 1. Note that the low porosity foam (88.9%) is prepared from a suspension with a larger solid content (higher starch/water ratio).

A lower preparation temperature (−27, −78, and −196 °C) will also result in smaller and more numerous cells, see Table 1. At higher heat removal rates and consequently larger degrees of undercooling, increased nucleation rates are obtained.[17] The growth rate will also decrease at large degrees of undercooling.[16,17] The ice crystal size will depend on both nucleation rate and growth rate.

Mechanical Properties. In Figure 2a, the compressive stress−strain curves for composite foams with varying MFC contents and similar densities are shown. The energy absorption of the foam is the area under the stress−strain curve. In Figure 2b, energy absorption diagrams are presented for the same materials in the form of absorbed energy per unit volume versus stress. This approach was presented by Maiti et al.[24] This type of diagram is useful in the design of packaging materials for a given application. In addition, experimental data can be combined with physical modeling, in order to improve the understanding of how biopolymers and cell structure influence biofoam properties. In Table 2, the mean values for Young's modulus, yield strength, relative density, and water content are summarized.

At low strains, the compressive stress−strain curves show linear elasticity and the plateau-like region that follows is due to collapse of the cells. At higher strains, opposing cell walls start to touch. This is termed the densification regime,[19] where the stress rises steeply with strain; see Figure 2a. In the energy absorption plot, Figure 2b, the densification regime is approached when the stress increases rapidly with a slowly rising energy per unit volume value.

The compressive stress−strain curves in Figure 2a and the results in Table 2 show that the Young's modulus, yield strength, and level of the plateau zone increased significantly with MFC content up to 40 wt %. At 60 and 70 wt % MFC content, a slight reduction in properties was observed. The mechanical properties of the foams depend both on the cell wall properties and the cell structure. With higher MFC contents, the anisotropy ratios generally decreased and the cell structure most likely contained a larger portion of open cells; these factors were the main reasons for the lower mechanical properties in the cylinder axis direction of the foam (the direction of the elongated cells). However, note that lower anisotropy ratios, have a positive effect on the mechanical properties in the orthogonal directions to the elongated cells (not measured here). The effect of MFC content on energy absorption is apparent in Figure 2b; the

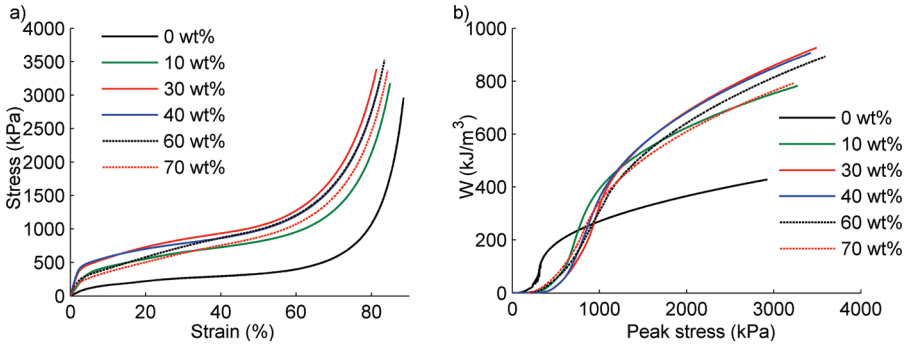

Figure 2. (a) Compressive stress−strain curves for composites with similar densities, preparation temperature (−78 °C) and varying MFC contents. (b) Energy per unit volume (W) versus peak stress, obtained for materials in panel a. Each curve is an average of five mechanical testing curves.

Table 2. Physical and Mechanical Properties of MFC Reinforced Amylopectin-Based Foams with Varying MFC Contents[a]

preparation T (°C)	MFC content (wt%)	density, ρ^* (kg/m^3)	relative density (ρ^*/ρ_s)	Young's modulus (MPa)	yield strength (kPa)	water content (%)
			Varying Cell Wall Composition (MFC/PAP)			
−78	0	108	0.088	3.4 (1.7)	130 (58)	11.7
	10	105	0.085	8.0 (2.2)	370 (51)	11.1
	30	113	0.089	18.3 (3.2)	440 (42)	10.3
	40	103	0.079	20.3 (5.1)	480 (105)	10.1
	60	102	0.076	11.9 (2.2)	280 (43)	9.3
	70	94	0.069	10.4 (0.8)	240 (11)	8.9
			Varying Preparation Temperatures			
−27	30	115	0.090	8.8 (1.9)	310 (59)	10.6
−78	30	113	0.089	18.3 (3.2)	440 (42)	10.3
−196	30	115	0.090	32.0 (10.6)	630 (72)	10.4
			Varying Foam Density (porosity)			
−78	30	52	0.041	2.6 (0.6)	64 (5.2)	10.3
	30	113	0.089	18.3 (3.2)	440 (42)	10.3
	30	157	0.12	54.1 (10.4)	1200 (170)	10.4

[a] The samples were conditioned in 51% RH and 23 °C for 3 days. The values within parentheses are the sample standard deviation.

energy per unit volume as a function of stress was approximately unchanged for MFC contents above 30 wt %.

In Table 2, the water content of the foams is presented. Evidently, the water content was reduced at elevated MFC content. This is expected, and mainly due to the less hygroscopic nature of cellulose nanofibers compared to amylopectin starch.[10,25]

In Figure 3, the stress−strain and energy absorption plots for composite foams with 30 wt % MFC content and almost identical densities are presented. The foams were prepared at three different temperatures; −27, −78, and −196 °C. By lowering the preparation temperature, smaller cell sizes and greater anisotropy ratios were generally attained, see Table 1. As a consequence, Young's modulus, yield strength and plateau level in the collapse region increased with lower preparation temperature, see Table 2. For foams in general, the Young's modulus value increases with higher cell anisotropy in the loading direction and is also enhanced by a larger proportion of closed cells.[19] Although details of the collapse mechanism are unknown for the present foams, rigid polymer foams at this relative density are expected to fail by plastic collapse.[19] Ashby's simple scaling laws for Young's modulus and plastic collapse in open or closed cell foams do not contain any influence from cell size. Still, because the real collapse mechanism is unknown, cell size may well have a direct effect. At this stage, the present data are probably best explained by reduced local cell wall stress because of the more favorable cell structure at smaller cell size (higher anisotropy and perhaps larger proportion of closed cells).

The results in Figure 3b demonstrate the potential to tailor the energy absorption capability of foam for a specific design peak stress, by simply varying the preparation temperature.

In Figure 4, the stress−strain curves and energy absorption data are depicted for composite foams with 30 wt % MFC content and different relative densities. The Young's modulus, yield strength and plateau level increased with relative density, as anticipated for polymer foams. The resulting energy absorption behavior in Figure 4b was also expected.[19] A change in cell shape anisotropy (see Table 1) was noticed in addition to the varying relative density, and this feature also had an effect on foam properties.

In Table 3, experimental data are presented for MFC reinforced biofoams from the current, as well as a previous study[10] and for expanded polystyrene.[26] The somewhat increased water content in foams of this study may lower the mechanical properties of the cell wall.[4,7] Still, the present 40 wt % MFC foam has a much higher modulus and comparable yield strength to the values obtained for the 40 wt % MFC foam in the past study, despite a less favorable cell shape anisotropy and larger moisture content. This is due to an increased proportion of closed cells attained by more careful

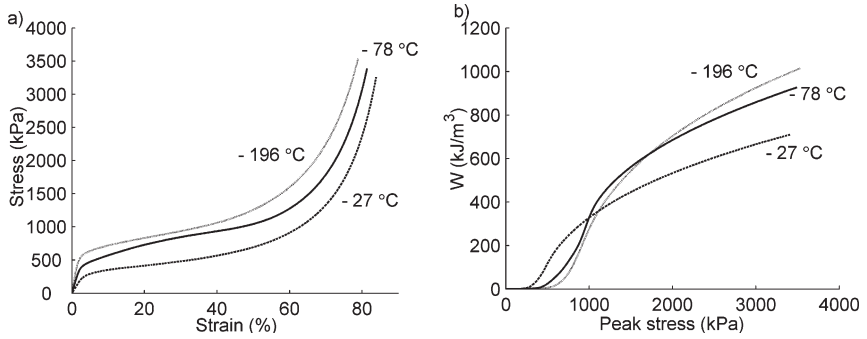

Figure 3. (a) Compressive stress−strain curves for composites with 30 wt % MFC content, identical densities and prepared at three different temperatures: −27, −78, and −196 °C. (b) Energy per unit volume (W) versus peak stress, shown for materials in panel a. Each curve is an average of five mechanical testing curves.

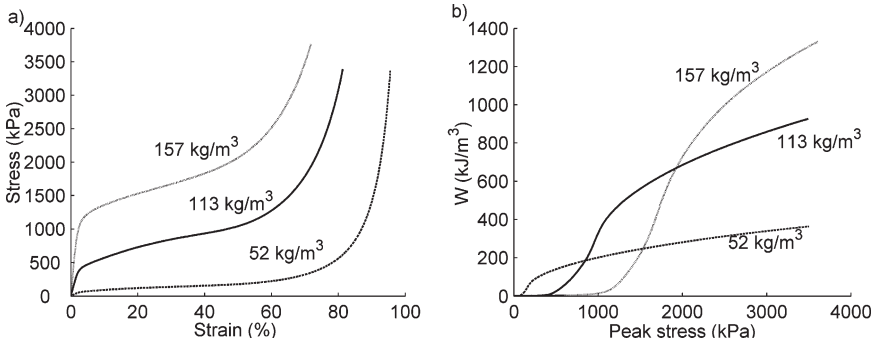

Figure 4. (a) Compressive stress−strain curves for composites with 30 wt % MFC content, and different densities. The foams were prepared at −78 °C. (b) Energy absorption per unit volume (W) versus peak stress. Each curve is an average of five mechanical testing curves.

Table 3. Mechanical Properties of MFC Reinforced Foams and Expanded Polystyrene

foam type	density, ρ^* (kg/m^3)	relative density (ρ^*/ρ_s)	Young's modulus (MPa)	yield strength (kPa)	water content (%)
amylopectin starch[a]	108	0.088	3.4	130	11.7
10 wt % MFC[a]	105	0.085	8.0	370	11.1
40 wt % MFC, old [b]	95.1	0.073	7.0	510	8.4
40 wt % MFC[a]	103	0.079	20.3	480	10.1
30 wt % MFC, −196 °C[a]	115	0.090	32.0	630	10.4
EPS (expanded polystyrene) [c]	100	0.095 [d]	48	620	----

[a] Data from present study. [b] Data after Svagan et al.[10] Compression test performed at 55% RH and 23 °C. [c] Data after Rinde et al. Compression test performed according to ASTM D1621.[26] [d] The density of the solid material, i.e., cell wall density, was 1050 kg/m^3.[19]

control of preparation conditions, such as the preparation temperature and freeze-drying temperature.[18] The yield strength does not improve for the present 40 wt % foam (480 vs 510 kPa), possibly because the yield stress of the cell wall itself is reduced by the higher water content.

The amylopectin starch foam shows less than 10% of the EPS modulus and about 20% of the yield strength. For EPS, the Young's modulus and yield strength were 48 MPa and 620 kPa, respectively. Rinde[26] reported that the cells were not elongated.

As a simplification, we may consider foams of the same relative density and with completely flat plateau regions, so that the yield strength is directly proportional to the total energy absorption of the foam. For this reason, we may regard the yield strength as a rough measure of energy absorption. Addition of 10 wt % MFC increases yield strength compared with neat starch foam by 3 times, but we are still only at half the value for EPS (370 vs 620 kPa).

The most successful composition in the present study is the 30 wt % MFC biofoam with an average modulus of 32 MPa and yield strength of 630 kPa. It means that a starch-based foam has for the first time shown mechanical properties very similar to EPS foam at comparable relative density and ambient conditions (50% RH). The reason is the cell wall reinforcement by a cellulose nanofiber network. The elongated cell structure obviously also contributes to the data. Still, if the cell structure can be improved further (more closed cells), energy absorption of cellulose nanocomposite biofoams will increase further.

CONCLUSIONS

For the first time, a starch-based biofoam was able to reach comparable mechanical properties (Young's modulus, compression yield strength) to expanded polystyrene at 50% relative

humidity. The reason was the cellulose nanocomposite concept in the form of a cellulose nanofiber network reinforcing the hygroscopic amylopectin starch matrix in the cell wall. It stabilized the moisture plasticized starch so that its inherent yield strength and modulus were not dramatically reduced. The hierarchical structure of the present biofoam was a challenge, since it is difficult to prepare cell wall reinforced biofoams with a large proportion of closed cells. In addition, cells may be elongated in the loading direction. Although this is positive from the mechanical property point of view, it requires greater effort when analyzing the effect of cell wall composition on foam properties.

Smaller cell size had a favorable effect on mechanical properties at the same relative density. Again, this was probably due to related cell structure changes, such as anisotropy and ratio of closed to open cells. Because plastic collapse was the most likely collapse mechanism of the present foams, it was not clear how cell size could influence compressive yield strength of the foam.

The effect of density on compressive stress−strain curves for the same cell wall composition followed expected trends. However, the cell structure changed with density and this also influenced the results.

Hierarchically structured biofoams are interesting materials with potential for strongly improved mechanical properties. The present study illustrated this and also highlighted the challenges involved in preparation and analysis of materials, which are structured at several different scales.

AUTHOR INFORMATION

Corresponding Author

*E-mail: svagan@kth.se (A.J.S.); blund@kth.se (L.A.B.). Tel: +46-8-7908118 (L.A.B.). Fax: + 46-8-7908101 (L.A.B.).

ACKNOWLEDGMENT

Financial support from the EU project Sustaincomp is gratefully acknowledged. In addition the SSF Biomime has provided support (A.J.S., L.A.B.).

REFERENCES

(1) Vincent, J. F. V. *J. Sci. Food Agric.* **1998**, *78*, 162.
(2) EUMEPS-European Association of EPS, Av. E. Van Nieuwenhuyse 4/3, B-1160 Brussels, Belgium, website: www.eumeps.org.
(3) Myllärinen, P.; Partanen, R.; Seppälä, J.; Forssell, P. *Carbohydr. Polym.* **2002**, *50*, 355.
(4) Dufresne, A.; Dupeyre, D.; Vignon, M. R. *J. Appl. Polym. Sci.* **2000**, *76*, 2080.
(5) Anglés, M. N.; Dufresne, A. *Macromolecules* **2000**, *33*, 8344.
(6) Anglés, M. N.; Dufresne, A. *Macromolecules* **2001**, *34*, 2921.
(7) Svagan, A. J.; Azizi Samir, M. A. S.; Berglund, L. A. *Biomacromolecules* **2007**, *8*, 2556.
(8) Henriksson, M.; Henriksson, G.; Berglund, L. A.; Lindström, T. *Eur. Polym. J.* **2007**, *43*, 3434.
(9) Favier, V.; Chanzy, H.; Cavaille, J. Y. *Macromolecules* **1995**, *28*, 6365.
(10) Svagan, A. J.; Azizi Samir, M. A. S.; Berglund, L. A. *Adv. Mater.* **2008**, *20*, 1263.
(11) Boccaccini, A. R.; Maquet, V. *Compos. Sci. Technol.* **2003**, *63*, 2417.
(12) Autissier, A.; Le Visage, C.; Pouzet, C.; Chaubet, F.; Letourneur, D. *Acta Biomaterialia* **2010**, *6*, 3640.
(13) Lebourg, M.; Suay Antón, J.; Gómez Ribelles, J. L. *Eur. Polym. J.* **2008**, *44*, 2207.
(14) Khan, F.; Walsh, D.; Patil, A. J.; Perriman, A. W.; Mann, S. *Soft Matter* **2009**, *5*, 3081.
(15) Jennings, T. A. *Lyophilization: Introduction and Basic Principles*; Interpharm CRC: Boca Raton, FL, 1999.
(16) O'Brien, F. J.; Harley, B. A.; Yannas, I. V.; Gibson, L. J. *Biomater.* **2004**, *25*, 1077.
(17) Kurz, W.; Fisher, D. J. *Fundamentals of Solidification*; Trans Tech Publications: Aedermannsdorf, Switzerland, 1986.
(18) Svagan, A. J.; Jensen, P.; Dvinskikh, S. V.; Furó, I.; Berglund, L. A. *J. Mater. Chem.* **2010**, *20*, 6646.
(19) Gibson, L. J.; Ashby, M. F. *Cellular Solids, Structure and Properties*; Cambridge University Press: Cambridge, U.K., 1997.
(20) DeHoff, R. T.; Rhines, F. N. *Quantitative Microscopy*; McGraw-Hill: New York, 1968.
(21) Hult, E.-L.; Iversen, T.; Sugiyama, J. *Cellulose* **2003**, *10*, 103.
(22) Ljungberg, N.; Bonini, C.; Bortolussi, F.; Boisson, C.; Heux, L.; Cavaillé, J. Y. *Biomacromolecules* **2005**, *6*, 2732.
(23) Tananuwong, K.; Reid, D. S. *J. Agric. Food Chem.* **2004**, *52*, 4308.
(24) Maiti, S. K.; Gibson, L. J.; Ashby, M. F. *Acta Metall.* **1984**, *32*, 1963.
(25) Svagan, A. J.; Hedenqvist, M. S.; Berglund, L. A. *Compos. Sci. Technol.* **2009**, *69*, 500.
(26) Rinde, J. A.; Hoge, K. G. *J. Appl. Polym. Sci.* **1971**, *15*, 1377.